論 文

[2113] AE Application to Fracture Mechanics

Masayasu OHTSU*

1. INTRODUCTION

The application of fracture mechanics to concrete materials is actively investigated to study the tensile and shear failure of concrete structures (1). The fracture mechanics is also of practical use for clarifying fundamental mechanisms of cracking. A critical stress intensity factor K_c was originally introduced as a fracture toughness parameter based on the linear elastic fracture mechanics (LEFM), whereas the applicability of LEFM to concrete is in debate. A major drawback of LEFM results from the presence of fracture process zone (2). To take into account the process zone, a cohesive crack model and a smeared crack model are proposed in the finite element method (FEM).

In the previous paper (3), the application of the boundary element method (BEM) to an analysis of crack propagation was studied, based on LEFM. Although crack traces predicted were in reasonable agreement with experimental findings, no care was taken with respect to the effect of the process zone. To confirm the feasibility of the previous procedure and to elucidate the length of the process zone, AE observation in a four-point-bending test of relatively small specimens is performed and plausible K_{Ic} values applicable to the prediction analysis of crack traces are investigated.

2. STRESS INTENSITY FACTOR AND FRACTURE PROCESS ZONE

An illustration near a crack tip in concrete is shown in Fig. 1. According to recent research, the fracture process zone is generated in front of a crack tip, where the bearing capacity of stress is finite. In LEFM, on the other hand, the stress concentration drawn in the figure is assumed. As a matter of course, actual stress distribution should be limited to the tensile strength, σ_t.

In spite of this drawback, LEFM can play a role for giving information on the orientation of crack propagation. Based on the criterion of maximum circumferential stress (4),

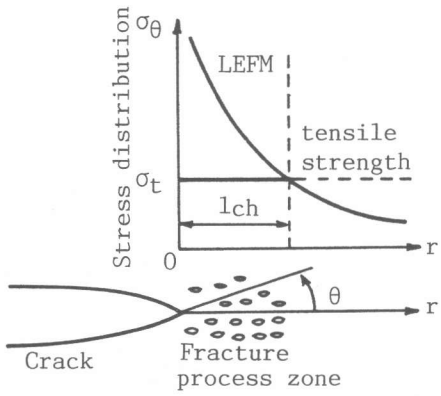

Fig. 1 Fracture process zone near a crack tip.

* Department of Civil and Environmental Engineering, Kumamoto University

the orientation θ (see Fig. 1) is determined as a solution of the following equation,

$$K_I \sin\theta + K_{II} (3\cos\theta - 1) = 0, \quad (1)$$

where K_I and K_{II} are stress intensity factors of opening mode and of in-plane shear mode, respectively. These two values at a crack tip can be theoretically calculated by the BEM analysis. Even though the effect of the process zone is taken into account, the criterion of eq. (1) is reasonably applicable. Because results of the other research on the pull-out tests (5) show that tensile microcracks in the early stage are mainly generated in parallel to the final failure surface. Therefore, when the configuration of the crack is prescribed in the BEM analysis, the orientation of crack propagation is readily determined from eq. (1).

In the next step, the criterion for crack initiation has to be studied. A criterion employed before is based on the use of the critical stress intensity factor of openning mode K_{Ic} (3), as follows;

$$\cos\theta/2 \, (K_I \cos^2\theta/2 - 3/2 \, K_{II} \sin\theta) > K_{Ic}. \quad (2)$$

Since the orientation and theoretical stress intensity factors are determined numerically, the determination of K_{Ic} has to be done from an experiment. It leads to the scope of the experiment for estimating K_{Ic} values, which are free from the effect of the fracture process zone.

In the present study, concrete specimens of normal size in a laboratory test and an ordinary loading machine other than stiffness loading are employed. In this case, it is known that the effect of the process zone is dominant at the final failure. One possibility to compensate the effect is to extrapolate results of small specimens into those of infinitely large specimens, based on the size effect law (6). Another procedure in the present paper requires the determination of K_{Ic} at the initiation of the process zone. It validates the condition of small-scale yielding in the small specimen. To identify the initiation of the process zone, the measurement of AE activity is employed.

3. EXPERIMENT AND ANALYSIS

Mix proportions for three different types of concrete are given in Table 1. These are labelled as MOR (mortar), AEC (air-entrained concrete with 5.9 % volume ratio of air), and SFR (steel reinforced concrete). For SFR specimens, steel fibers of dimension 0.5 mm x 0.5 mm x 30 mm were mixed at 1 % volume ratio. Summarized in Table 1 are the compressive strength,

Table 1 Mix proportion and mechanical properties

Type	Unit weight (kg/m^3) water	cement	sand	gravel	Compressive strength(Mpa)	Tensile strength(Mpa)	Young's modulus(Gpa)
MOR	353	589	1178	-	28.1	1.76	19.3
AEC	169	375	695	1156	33.7	2.88	28.4
SFR	169	375	684	1138	45.0	5.10	31.5

the tensile strength, and Young's modulus. These are the averaged results of three cylindrical specimens of 10 cm diameter and 20 cm height.

A notched beam for a four-point bending test is of dimension 10 cm x 10 cm x 40 cm. A notch was made by inserting a plastic plate of 1 mm thickness into a mould. Notch depths designed are 2 cm, 3 cm, and 5 cm. For the notch depth = 3 cm, another specimen with a steel plate of 3 mm thickness and an apex angle 30^{o} inserted was cast to compare the effect of the notch shape.

Four-point bending tests were carried out in the similar way to the previous paper (3). AE events were detected by an AE sensor attached at a location of 1 cm apart from the notch tip, and were monitored through a pre-amplifier, a discriminator, and a counter. Total amplification was 60 dB and the frequency range was 10 kHz to 300 kHz. The threshold level for counting was set at 120 mV. The crack-mouth displacement (CMD) was also measured by using a clip gauge.

The BEM analysis was performed for the elastic stress analysis. The program is the same as the other research (5), which implements a constant-element formulation.

A sketch of the model near the notch tip is shown in Fig. 2. Boundary nodes of elements and internal points for the stress analysis are indicated. Note that the configuration of the notch tip is modelled as similar as the inserted plate. In the computation, Young's modulus obtained in Table 1 was employed for each mix type, while Poisson's ratio was set to 0.2 in all mix proportions. The stress distributions on the ligament and at internal points were determined by the BEM analysis.

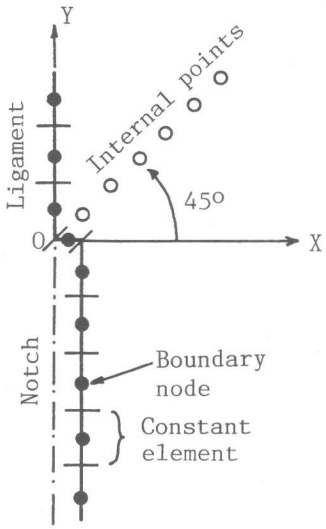

Fig. 2 BEM model near a crack tip.

Because the notch tip is not exactly of edge shape and could be blunted due to microfracturing in concrete, the stress intensity factors were determined from a linear extrapolation of K_I values at internal points, besides from the well-known formula. The linear extrapolation is based on the least square error estimation.

4. RESULTS AND DISCUSSION

The critical stress intensity factor, K_{Ic}, is conventionally determined from a mathematical formula,

$$K_{Ic} = P_{cr}L(a)^{0.5}Y^{*}/(BD^{2}), \tag{3}$$

where P_{cr} is the failure load, L is the span length, a is the notch depth, B is the specimen width, and D is the beam depth. Y^{*} is the shape function for the notched beam. Substituting values of failure loads into eq. (3), K_{Ic} values are determined. Results are indicated in Table 2 as $K_{Ic}(P_{cr})$. These values are the averaged results of two specimens. In the table, the case of the steel-plate notch is denoted as S3. It is found that the notch shape affects considerably K_{Ic} values except for MOR specimens.

From Fig. 1, it is considered that the fracture process zone approximately corresponds to the region where elastic stress is greater than the tensile strength. Stress component σ_{xx} near the crack tip is represented as,

$$\sigma_{xx} = K_I \cos\theta/2\ (1 + \sin\theta/2 \sin 3\theta/2)/(2\pi r)^{0.5}. \quad (4)$$

In the case $\theta = 0$, it holds that $K_I = (2\pi r)^{0.5} \sigma_{xx}$. In the last form, substituting the critical value K_{Ic} and the tensile strength σ_t into K_I and σ_{xx}, a characteristic length,

$$l_{ch} = [k_{Ic}/\sigma_t/(2\pi)^{0.5}]^2, \quad (5)$$

is determined. These values are denoted as $l_{ch}1$ in Table 2. Although several characteristic lengths are propopsed on the basis of the fracture energy absorption (4), the physical meaning of the present l_{ch} is simple. It corresponds to the distance apart from the notch tip, at which location the stress level is considered to surpass the tensile strength, assuming that the principle of LEFM holds.

To consider elastic stress near the notch tip, the case of an AEC specimen with 2 cm notch depth is shown in Fig. 3. The upper graph shows the stress distribution on the ligament and at internal points determined from the BEM analysis. Observing the case of applying the load P_{cr}, the location where the stress curve on the ligament intersects the tensile strength (2.88 Mpa) is nearly 5 mm apart from the notch tip, while the corresponding $l_{ch}1$ in Table 2 is 6.55 mm. It implies that the characteristic length $l_{ch}1$ is over-estimated in LEFM, because the process zone is already developed to some amount at the failure load. Therefore, K_{Ic} values in Table 2 are not applicable to eq. (2).

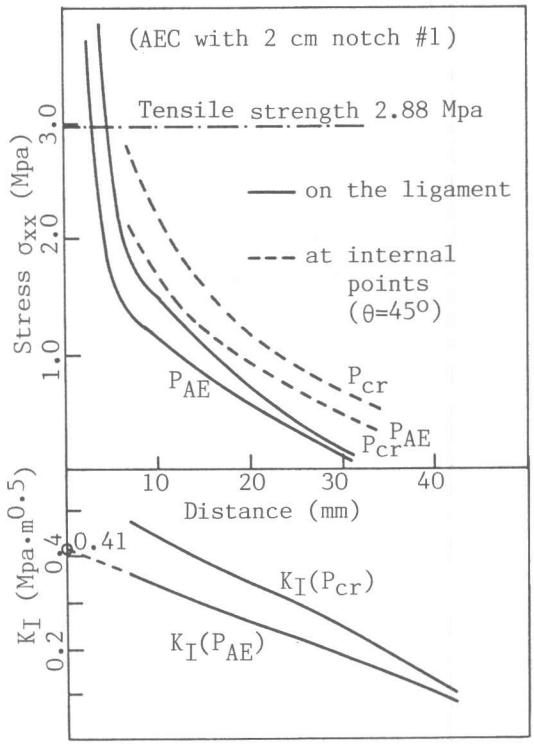

Fig. 3 Stress distribution near a crack tip by BEM.

To utilize eq. (2) for the prediction of crack traces, the load level where the process zone starts to be nucleated should be reasonably identified. To this end, AE activity and the crack-mouth displacement (CMD) were measured during experiments. The case of the AEC specimen with 2 cm notch is shown in Fig. 4. It is observed that both total AE counts and the CMD values acceleratedly increase at a certain load level, which is indicated by an arrow as P_{AE}. In the previous study (3), although this load levels were employed to determine K_{Ic} values, the CMD measurement was not performed. By combining with the CMD measurement, the load level P_{AE} is readily assigned from the figure.

To determine plausible K_{Ic} values, another BEM analysis was performed,

based on the load levels P_{AE}. Results of the stress analysis applying the load P_{AE} are also plotted in the upper graph of Fig. 3. The considerable decrease of the stress distribution is observed.

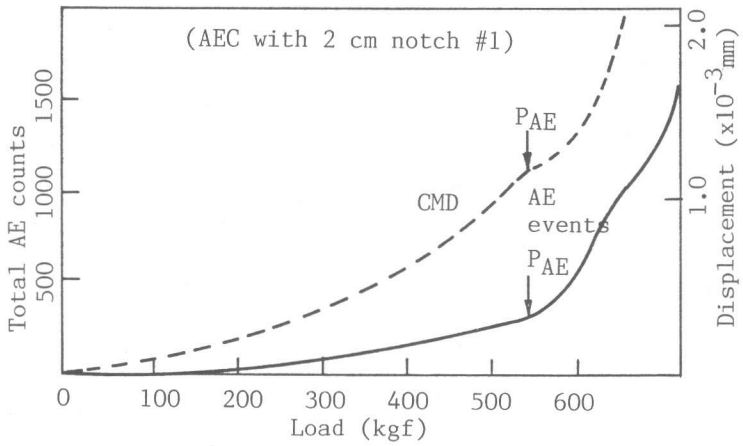

Fig. 4 AE activity and CMD in an AEC specimen with 2 cm notch.

Since the nothch tip in concrete should be blunted under loading, the applicability of eq. (3) for the determnination of K_{Ic} values is in doubt. Consequently, K_I values are determined by the extrapolation. Applying load P_{AE} in the BEM model, K_I values were determined at internal points on the basis of eq. (4). Then, these are approximated by the equation, $K_I = A \times r + K_{Ic}$, on the basis of the least square method. Extrapolating into a value at the crack (r tends to 0), the critical stress intensity factor K_{Ic} is obtained. An example is shown in the bottom of Fig. 3, where the critical value 0.41 Mpam$^{0.5}$ is indicated. In the same figure, the K_I plots in the case of P_{cr} are also shown.

Table 2 Critical stress intensity factor and characteristic length

Type	Notch depth (cm)	$K_{Ic}(P_{cr})$ (Mpam$^{0.5}$)	l_{ch}^1 (mm)	$K_{Ic}(P_{AE})$ (Mpam$^{0.5}$)	l_{ch}^2 (mm)
MOR	2	0.33	5.50	0.26	3.39
	3	0.34	5.94	0.24	2.99
	S3	0.33	5.47	0.23	2.77
	5	0.40	8.25	0.19	1.88
AEC	2	0.58	6.55	0.41	3.18
	3	0.56	6.04	0.37	2.66
	S3	0.52	5.20	0.32	1.95
	5	0.54	5.68	0.25	1.22
SFR	2	0.95	5.33	0.49	1.47
	3	0.86	4.51	0.48	1.41
	S3	1.00	6.15	0.48	1.41
	5	0.89	4.88	0.47	1.36

Determined K_{Ic} values in the present procedure are shown in Table 2 as $K_{Ic}(P_{AE})$. It is interesting that the effect of the notch shape is not so dominant in these cases as seen in the conventional cases.

Thus, in the same as before, characteristic length l_{ch} is determined from $K_{IC}(P_{AE})$ and σ_t. Results are shown as $l_{ch}2$. From Fig. 3, it is known that the region where the stress surpasses the tensile strength due to the load P_{AE} is apart from approximately 3 mm. This length is comparable to $l_{ch}2$ (3.17 mm). It suggests that the discrepancy between LEFM and the actual stress condition is not so considerable as in the conventional procedure. Therefore, it is considered that the effect of the process zone is not dominant on K_{Ic} values determined from loads P_{AE}.

In SFR specimens, K_{Ic} values seem independent of the notch depths. It may be due to the high toughness of fiber-reinforced concrete. In AEC and MOR samples, K_{Ic} values are fairly stable except for the case of 5 cm notch. In the case of small specimens of low toughness, the extension of the fracture process zone on the ligament is considered to occur abruptly. An unstable collapse may be observed. This is the reason why K_{Ic} values are determined as low values in the 5 cm notch, which corresponds to a half of the beam depth. In other words, it implies that the size effect is still dominant in the cases of AEC and MOR specimens with 5 cm notch, even though the present procedure is applied.

5. CONCLUSION

The scope of the research is to estimate the critical value K_{Ic} for the initiation of the process zone, because the procedure for the prediction of crack traces is under development. The feasibility of the values is investigated in respect to the characteristic length, which is determined from the K_{Ic} value by AE observation and the tensile strength. Results show that for high toughness materials, the present procedure based on AE observation and LEFM is available.

ACKNOWLEDGEMENT

The author wishes to thank Messers. S. Sawai and T. Yano for their valuable collaboration in experiments and the analysis. It is also stated that a part of this research is financially supported by the Grant-in-Aid for Scientific Research (c), the Ministry of Education, NO. 62550349.

REFERENCES

1) "Proc. of International Workshop on Fracture Toughness and Fracture Energy-Test Methods for Concrete and Rock," Tohoku University, 1988.
2) Sih, G. C. and DiTommaso, A. eds.,"Fracture Mechanics of Concrete," Martinus Nijhoff Publication, 1985.
3) Ohtsu, M.,"Crack Propagation in Concrete: Linear Elastic Fracture Mechanics and Boundary Element Method," Theoretical and Applied Fracture Mechanics, Vo. 9, No. 1, 1988, 55-60.
4) Carpinteri, A. "Mechanical Damage and Crack Growth in Concrete," Martinus Nijhoff Publication, 1986.
5) Ohtsu, M. and Shigeishi, M. and Iwase, H.,"AE Observation in the Pull-out Process of Shallow Hook Anchors," Proc. JSCE (in press).
6) Bazant, Z. P. and Pfeiffer, P. A.,"Determination of Fracture Energy from Size Effect and Brittleness Number," ACI Materials Journal, 1987, 463-480.